



Research article

Temperature prediction and analysis based on improved GA-BP neural network

Ling Zhang, Xiaoqi Sun* and Shan Gao

School of Mathematics and Statistics, Qingdao University, Shinan District, Qingdao, Shandong, China

* **Correspondence:** Email: sunxiaoqi@live.com; Tel: +8613793263882.

Abstract: In order to predict the temperature change of Laoshan scenic area in Qingdao more accurately, a new back propagation neural network (BPNN) prediction model is proposed in this study. Temperature change affects our lives in various ways. The challenge that neural networks tend to fall into local optima needs to be addressed to increase the accuracy of temperature prediction. In this research, we used an improved genetic algorithm (GA) to optimize the weights and thresholds of BPNN to solve this problem. The prediction results of BPNN and GA-BPNN were compared, and the prediction results showed that the prediction performance of GA-BPNN was much better. Furthermore, a screening test experiment was conducted using GA-BPNN for multiple classes of meteorological parameters, and a smaller number of parameter sets were identified to simplify the prediction inputs. The values of running time, root mean square error, and mean absolute error of GA-BPNN are better than those of BPNN through the calculation and analysis of evaluation metrics. This study will contribute to a certain extent to improve the accuracy and efficiency of temperature prediction in the Laoshan landscape.

Keywords: temperature prediction; genetic algorithm; BP neural network; neural network optimization

1. Introduction

Temperature changes are influenced by many factors. Different regions have different topography, altitude, latitude and longitude, which can lead to different temperatures. Meanwhile, the intensity of solar radiation, changes in the Earth's orbit, and anthropogenic factors caused by human activities can also cause temperature variations. We currently have a wide variety of temperature-related data. How to effectively apply these meteorological data for accurate temperature prediction became an issue to be resolved. In addition, human productive life depends heavily on changes in temperature. It has

a huge impact in the fields of agriculture, animal husbandry, aquaculture, tourism and transportation. We need to adjust our various activities in time according to the different temperatures. Therefore, it is necessary to select relevant data more efficiently for more accurate temperature prediction.

Current research on weather forecasting issues has gained the attention of researchers. Khaniani et al. [1] compared the prediction effectiveness of two types of neural networks by selecting multiple classes of meteorological parameters. Huang et al. [2] established a fuzzy time series model based on automatic clustering interval differentiate method to predict the precipitation in spring, summer, autumn and winter in Xinjiang. Lee et al. [3] developed an artificial neural network(ANN)-based regional rainfall forecast model suitable for the Geum River Basin in South Korea, using teleconnection climate indices. In [4], Liu et al. proposed a class of multi-meteorological parameter short-term rainfall forecasting models based on improved BPNN algorithm design for precipitation prediction in Singapore. Taking the prediction of precipitation in the Chao River Basin as the research object, Guan et al. [5] compared two methods, kriging interpolation method in GIS program and constructing BPNN. It showed the higher usefulness of BPNN model in weather prediction. Peng et al. [6] proposed a deep neural network (DNN) hyperparameter auto-optimization method that can automatically optimize the hyperparameters of DNNs. It makes the precipitation prediction problem more convenient for people to operate. For the post-processing problem of numerical weather prediction, Cho et al. [7] proposed a new multi-model ensemble. Shi et al. [8] proposed a cyclic evolutionary network model (CENS) consisting of multiple network node units that can automatically match data from different regions to the appropriate network node unit. Working with the RegCM4 ensemble, in [9], as well as the Bayesian model averaging (BMA) weights, Song et al. investigate the temperature prediction problem for 88 climate stations in Canada.

Most of the above works have adopted the ANN approach for weather prediction, especially in [4, 5] the BP neural network model was utilized. Due to its highly nonlinear mapping capability and generalization ability, bp neural networks have been deployed in many fields. However, there are certain shortcomings of BP neural networks in terms of prediction. For example, long training time, over-fitting phenomenon and the tendency to fall into local extremum. This would lead to the connection weights and thresholds not being optimal. As a result, the error of prediction increases.

Recently, the study of genetic algorithms has been focused on various research areas (e.g., optics, IoT security, traffic scheduling, power systems, mechanical design, etc. [10–14]). Because of its global optimization capability, genetic algorithms have been used for prediction problems. In [11], a multi-model integrated forecast experiment about temperature in the Jiangnan area (26° – 31° N, 112° – 121° E) was conducted using linear ensemble methods such as weighting, regression, and bias-removed, combined with GA-BP neural network. Yao et al. [12] applied GA to model the prediction of tropical cyclone intensity in the South China Sea by sifting factors, which made the prediction more stable. In [13], the Simulated Annealing algorithm (SA) was combined with (GA) to propose a HGASA-NN model for daily precipitation prediction. Tang et al. [15] proposes a class of GA-BP neural networks for the air quality index (AQI) prediction problem during the winter heating period.

The general prediction model first trained the structure of the neural network. In this study, the optimal weights and thresholds of the network were first found by genetic algorithm. Combined with the geographical environment of Laoshan scenic area, the day-by-day meteorological data between 2021 and 2022 were selected for the prediction experiment. By comparing each prediction result index

of the improved model with the original model, it is shown that the prediction data of the improved model is closer to the actual data.

The remainder of this paper is organized as follows. In Section 2, relevant preliminary knowledge of BP neural network and genetic algorithm is given, and the GA-BPNN prediction model of this study is proposed. In Section 3, the prediction simulation experiments of BPNN and GA-BPNN are conducted separately using the obtained meteorological data of Laoshan scenic area, and the prediction results are compared. In Section 4, the GA-BPNN is further used to do the screening of 9 types of meteorological data, which in turn leads to efficient prediction with less data. Finally, Section 5 concludes the paper.

The main contributions of this paper are as follows. For the temperature prediction problem of Laoshan scenic area in Qingdao, an improved GA-BPNN is proposed, and the weights and thresholds of the neural network are optimized using GA to improve the accuracy of prediction. The GA-BPNN is used to conduct screening test experiments on multiple types of meteorological parameters in Laoshan scenic area to improve the prediction efficiency.

2. Problem modeling

2.1. BP neural networks

BP neural networks are a class of networks that learn by back propagation. It contains three layers of structure, which are input layer, implicit layer and output layer. BPNN gradually adjusts the input weights between layers through the training error. This adjustment process uses a gradient descent algorithm. If the output error of the sample does not match the preset convergence error, then the network will iteratively computed by backpropagation. The iterative process causes the parameter values among the connected layers to be modified so that the error is reduced. The iteration ends when the error is reduced to the target value.

The actual computational output equation of this model is:

$$\hat{y}_j = \mathcal{S} \left(\sum_{i=1}^p b_i \varpi_{ij} + \gamma_j \right), \quad (2.1)$$

where b_i is the activation values for the i -th input to the j -th output; ϖ_{ij} is connecting weighting coefficients, at the initial moment it is a random small quantity; γ_j is the output layer unit threshold; \mathcal{S} is the sigmoid function that is $\mathcal{S}(s) = \frac{1}{1+e^{-s}}$.

2.1.1. Genetic algorithm

The concept of genetic algorithm was first introduced by Holland in 1962. The algorithm models the mechanism of biological evolution and is a process search algorithm. The genetic algorithm first considers the parameters as gene fragments and encodes them. Subsequently, the sub-generation will undergo selection, crossover and mutation to exchange the information carried on the gene fragments and eventually generate chromosomes that meet the desired conditions.

The first step of the algorithm is the initialization of the population. It generates the initial population by selecting a suitable encoding method to transform multiple sets of solutions (in the solution set) into chromosomes which carry various data information. By selecting the fitness function, the individual's fitness is assessed. Fitness is the extent to which species in nature are

matched to their environment. By evaluating individuals in the population, the algorithm selects individuals that fit the survival environment to continue reproducing, so that the good genes can be kept alive. (2.2) is the fitness function

$$U = k \left[\sum_{i=1}^p |y_i - o_i| \right], \quad (2.2)$$

where, p for network with p nodes; y_i denotes the expected value at the i -th node; o_i indicates the actual output on the i -th node and denote the parameter by k . The next step of the algorithm performs the selection operation. This step will pick the genes that are beneficial to the survival of the individual from the many genes carried by the chromosomes. To allow the selected genes continue to exist in the next generation. If the value of fitness for each member i is denoted as U_i , then let $\mathfrak{I}_i = \frac{k}{U_i}$, where k is a parameter, individual i 's probability of selection v_i can be expressed as (2.3)

$$v_i = \frac{\mathfrak{I}_i}{\sum_{i=1}^N \mathfrak{I}_i}, \quad (2.3)$$

N denotes quantity of the individuals in the species. Next, perform crossover. Crossover is the main method of generating new individuals, which represents the idea of information exchange. It interchanges some genes and forms new combinations to construct filial generation. (2.4) represents the expression for the crossover of chromosomes k and l at the j -th position

$$\begin{cases} \sigma_{kj} = \sigma_{kj}(1 - b) + \sigma_{lj}b \\ \sigma_{lj} = \sigma_{lj}(1 - b) + \sigma_{kj}b. \end{cases} \quad (2.4)$$

Then perform variation. During the reproduction of offspring, genetic information can be wrong with some probability, resulting in offspring with different chromosomal expression information than the previous generation. If we use σ_{max} to denote up-bound of the gene σ_{ij} and σ_{min} to denote down-bound of the gene σ_{ij} , then (2.5) represents the mutation operation of the gene σ_{ij} .

$$\sigma_{ij} = \begin{cases} \sigma_{ij} + (\sigma_{ij} - \sigma_{max}) \cdot \psi(\eta) & \rho > 0.5 \\ \sigma_{ij} + (\sigma_{min} - \sigma_{ij}) \cdot \psi(\eta) & \rho \leq 0.5, \end{cases} \quad (2.5)$$

where $\psi(\eta) = \rho \cdot \left(1 - \frac{\eta}{\mathcal{G}_M}\right)^2$, $\rho \in [0, 1]$ is generated randomly; η means present iteration numbers; \mathcal{G}_M means the maximum number of evolutions.

2.2. GA-BP neural network prediction model

BPNNs can predict samples by training the network, which has led many scholars to use BP neural networks to study weather prediction problems. However, BP neural networks are not perfect in prediction. This is due to the arbitrary settings of initial values, number of nodes and weights of BP neural networks and the limitations of the gradient descent method. These problems cause the algorithm to produce local extremes, which affect the efficiency of the operation and make the predicted values less accurate. The shortcomings of BPNN are compensated, in this study, by using

improved genetic algorithm to reduce the arbitrariness of network parameter setting. Thus, the purpose of improving the accuracy of prediction is achieved.

By genetic manipulation, as shown in Figure 1, the individual fitness values will be evaluated and the most adapted individual will be found. The advantage of this approach is that the network can get the optimal parameters, which results in more accurate predicted values.

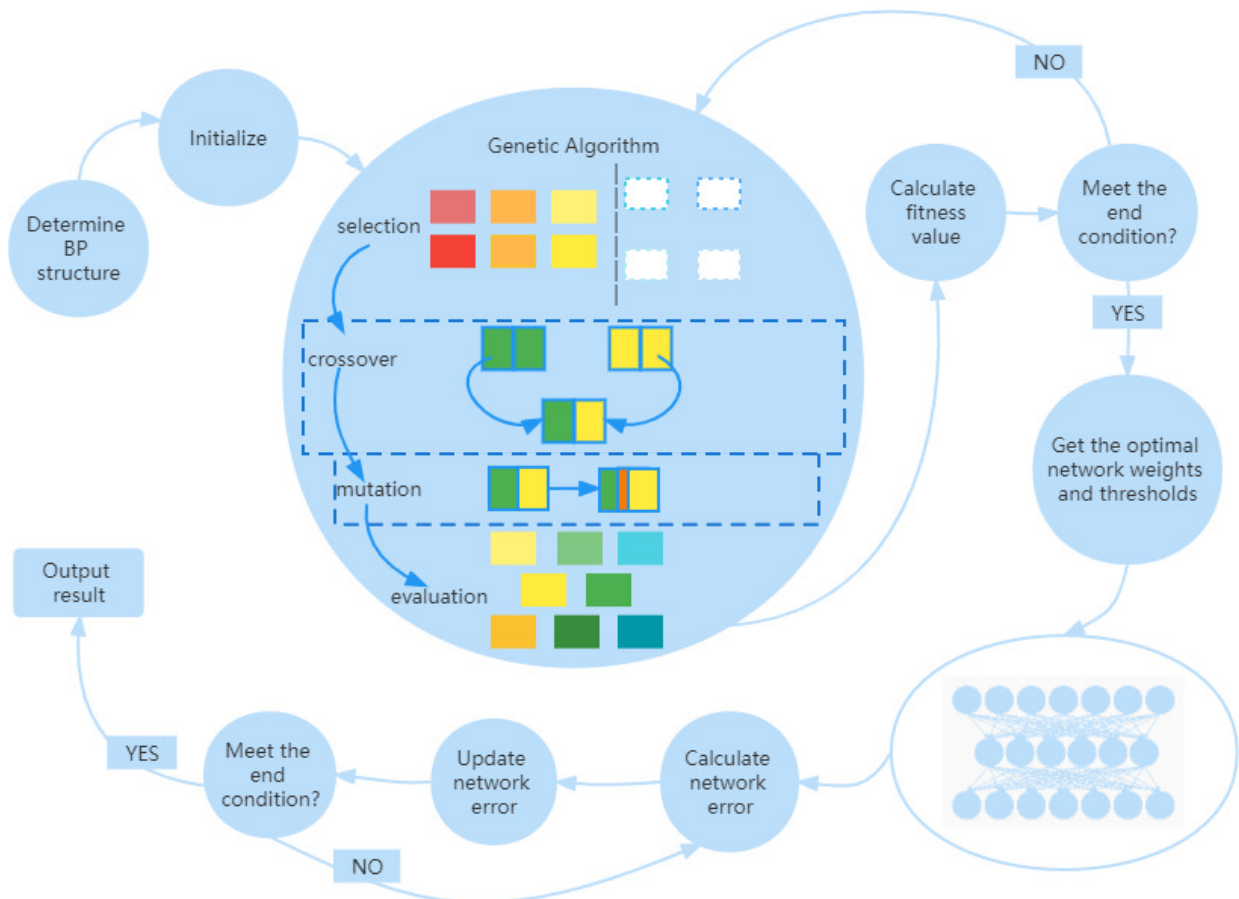


Figure 1. The flow chart for GA-BP neural network algorithm.

3. Simulation experiments

3.1. Data presentation and processing

In this paper, the meteorological data from January 1, 2021 to February 4, 2022 for the Laoshan Scenic Area ($36^{\circ}05' - 36^{\circ}19' \text{ N}$, $120^{\circ}24' - 120^{\circ}42' \text{ E}$) were selected as simulation data. The data was obtained from the website <https://rp5.ru>. The meteorological data were recorded every 3 hours in the raw data, and the data were measured 8 times a day, with a total of 3200 data sets of samples. There are 15 types of data including the number of clouds and snow depth on this website. According to the

geographical location and climatic characteristics of Laoshan Scenic Area, we selected horizontal air pressure (HAP), mean sea level pressure (MSLAP), 2 meters (above the horizontal) relative humidity (RH), and mean wind speed (MWS) (about 10 meters above the horizontal), 10–12 meters maximum gust between observations (MAXG), minimum air temperature between two observations (MINT), horizontal visibility (HV), and 2 meters above ground dew point temperature (D-PT) as the input of this experiment. For further simplification, we calculated the daily average of the data for eight times a day, and finally obtained 400 sets of data samples. The high autocorrelation of the input variables may cause overfitting phenomenon, which affects the model prediction accuracy. In this study, the data were initially processed using pauta criterion [16] (i.e., when the absolute value of the difference between a measurement and the mean is greater than 3 standard deviations, the measurement is considered an outlier, and the value is replaced with the mean of the data on both sides of the outlier).

Further, there are differences in the units of the parameters. For example, the value of horizontal atmospheric pressure is around 765 mmHg, while the relative humidity is in the range of 50%–60%. To avoid the influence of these differences on the prediction results, we normalized the data using *Matlab* and the normalization function used was *mapminmax*(·). This function normalizes all data to between $[-1, 1]$. The parameters after partial normalization are listed in Table 1.

Table 1. Normalized data.

HAP	MSLAP	RH	MWS	MAXG	MINT	HV	D-PT
0.8090	0.8045	0.1840	0.0327	0.1217	0.2614	0.6474	0.2361
0.8865	0.8786	0.3810	0.0981	0.0609	0.2875	0.3388	0.3350
0.9493	0.9393	0.7175	0.0327	0.0000	0.3332	0.1016	0.4207
0.9047	0.8960	0.7175	0.2290	0.1565	0.3521	0.0646	0.4254
0.9879	0.9792	0.3086	0.5724	0.5130	0.2841	0.7576	0.2322
0.8978	0.8948	0.2305	0.6542	0.8174	0.1900	0.7752	0.1459
⋮	⋮	⋮	⋮	⋮	⋮	⋮	⋮
0.9398	0.9185	0.2361	0.3598	0.8696	0.6230	0.9295	0.4775
0.9177	0.9002	0.2026	0.1308	0.3217	0.5361	1.0000	0.4556

3.2. The network structure design

After several Matlab numerical experiments, among 400 sets of sample data, the first 290 sets were used as training samples and the last 110 sets were used as prediction samples. The selection of the number of nodes in the hidden layer is one of the factors that affect the model prediction. Too few nodes will affect the learning of the network and increase the training times; too many nodes will prolong the training time and make it easily overfitted. The scope of the number of implied layers is determined in this paper using Eq (3.1).

$$n = \sqrt{n_i + n_o} + q, \quad (3.1)$$

which n_i stands for the nodes of the input layer; n_o means the nodes of the output layer; $q \in [1, 10]$ is a constant. In this paper, the input data of the simulation experiment is 8 and the output data is 1. From the above equation, the range of the number of nodes is $[4, 13]$. The results of RMSE corresponding to different number of nodes are shown in Table 2.

Table 2. Root mean square error of BP neural networks with different number of hidden layer nodes.

n	4	5	6	7	8	9	10	11	12	13
RMSE	0.9562	0.5755	0.9570	1.1449	0.8136	0.5289	0.8157	1.1014	1.319	1.7056

From Table 2, we can conclude that the number of nodes is 9 and the corresponding RMSE value is the smallest.

With the aim of obtaining the best results for prediction, in addition to the single hidden layer, this study tried to set the two-hidden-layer. Through the experiments we found that the double hidden layers made the network structure more complicated and took longer time for the experiments. And it did not make the network show better prediction. Table 3 shows the experimental parameters recorded during the prediction tests for the single and double models. The number of hidden layer nodes set during the tests were all 9.

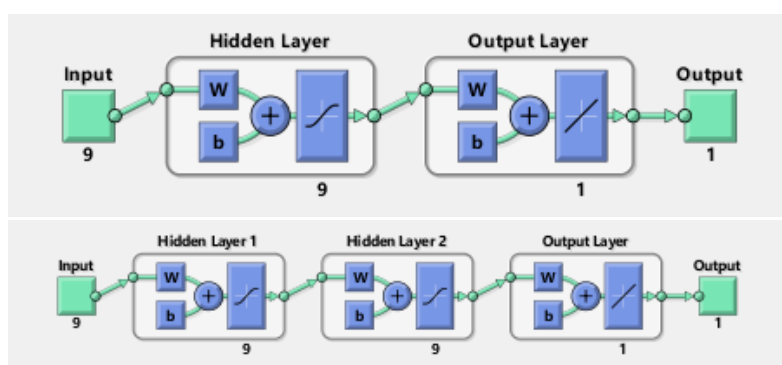


Figure 2. Single and double hidden layer BPNN structure diagram.

Therefore by comparison this paper choice to use single hidden layer BPNN. And the structure of the BP neural network is $8 - 9 - 1$. So the number of weights is $8 \cdot 9 + 9 \cdot 1 = 81$, and the number of thresholds is $9 + 1 = 10$.

Table 3. Operating parameters of BPNN with single and double hidden layer.

Number of hidden layers	Running time	Root mean squared error (RMSE)	Mean absolute error (MAE)	Mean absolute percentage error (MAPE)	R-squared (R^2)
Single	16.285604	0.82121	0.6268	34.0871	0.98438
Double	19.568335	1.5751	1.1846	120.6385	0.94286

3.3. BPNN temperature prediction and result analysis

As an artificial intelligence-like learning scheme, BP neural network is realized by using repeated training samples. Only by using original samples for high-quality training can obtain excellent training results, which in turn determines the quality of neural network predictions. In this paper, Matlab software is used to implement the BP neural network. In the early stage of training, the original samples

are standardized and converted. The minimum training rate is set to 0.01, the maximum number of iterations is set to 50 during the training process control, and the allowable error is set to 0.0001. The fitting between the predicted and measured values of BPNN training is shown in Figure 3. The change trend of the training predicted value and the measured value is basically the same. Figure 4 shows the temperature prediction result curve and the temperature prediction error curve of the test sample after training.

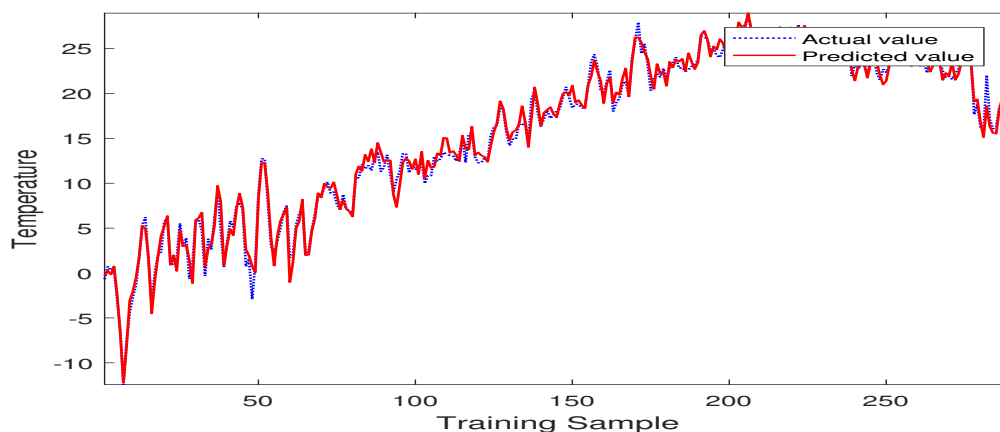


Figure 3. Training curve of BP neural network.

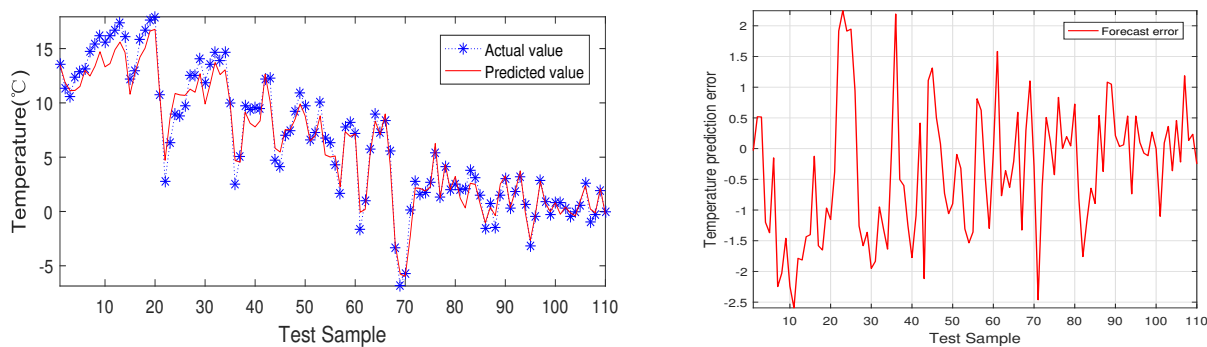


Figure 4. Temperature prediction results and the error curve of BP neural network.

3.4. Temperature prediction based on GA-BP neural network

As an algorithm to randomly find the global optimal solution, the genetic algorithm can find the globally optimal link weight and threshold of the BP neural network, thereby avoiding the defects of the traditional BP neural network. In this section, according to the process shown in Figure 1, GA-BPNN is used to predict the temperature of Laoshan Scenic Area. Settings of the experimental parameters for GA are shown in Table 4.

Table 4. Parameter setting of GA.

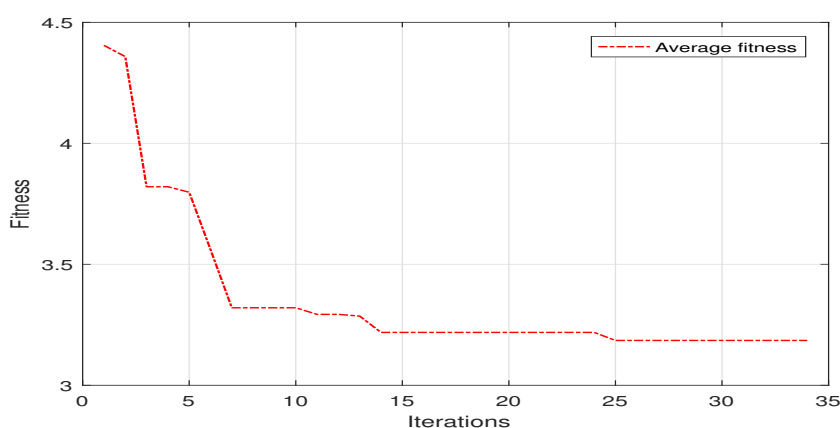
Individual coding length	Population size	The number of evolution	Crossover probability	Variation rate
100	50	100	0.4	0.001

Table 5. Optimal initial weights and thresholds.

Input-hidden layer weights (81)	Implicit-output layer weights (9)	Hidden layer node thresholds (9)	Output layer node thresholds (1)
-0.3208	-0.6306	0.3491	-0.8122
0.3562	0.6992	-0.9190	–
0.7714	-0.2670	-0.3955	–
0.5480	-0.0619	0.7009	–
0.4451	-0.1482	0.0497	–
⋮	-0.6716	0.4268	–
-0.5893	0.8712	-0.9005	–
-0.0489	0.2260	-0.2524	–
-0.6791	-0.8542	0.7660	–

The optimal individual with the best fitness is found by the optimization-seeking operation of the GA. The weights and thresholds of the network were updated after the optimization by the genetic algorithm. The relevant data are given in Table 5.

Figure 5 shown the fitness evolution curve. It is derived that the average fitness value, in Figure 5, decreases most rapidly when the number of evolutionary generations is between 0–10 generations; when it is between 10–25 generations, the average fitness value decreases flatly; after 25 generations, the average fitness value maintains a stable state.

**Figure 5.** Fitness evolution curve.

It is derived that the average fitness value, in Figure 5, decreases most rapidly when the number of evolutionary generations is between 0–10 generations; when it is between 10–25 generations, the average fitness value decreases flatly; after 25 generations, the average fitness value maintains a stable state.

After training the network by performing 100 iterations on the normalized data, the resulting fitted curve and error curves is shown in Figure 6.

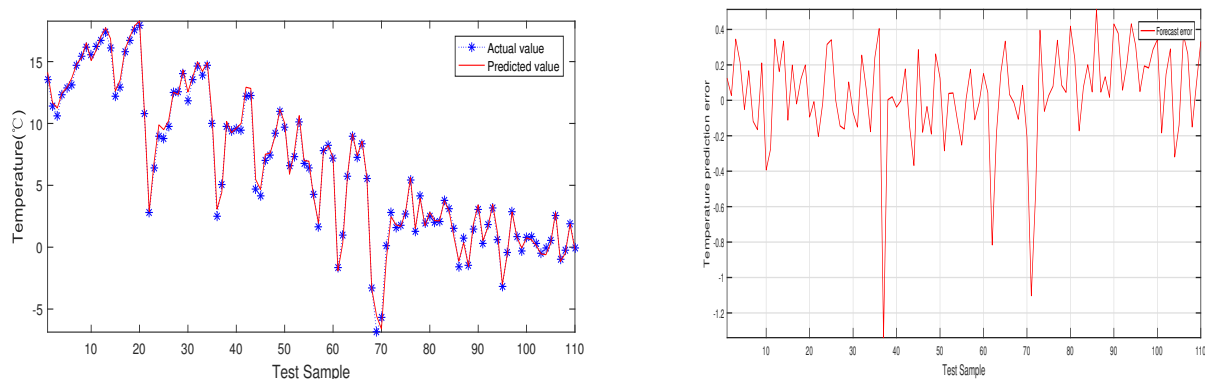


Figure 6. Temperature prediction results and the error curve of GA-BPNN.

3.5. Comparative analysis of BPNN and GA-BPNN

For a more intuitive analysis and comparison of the prediction performance of BP and improved GA-BP networks more intuitively, we plotted the fitting curves based on the prediction result data separately.

In order to more intuitively analyze and compare the prediction performance of BP network and improved GA-BP network, we plot the fitting curves based on the prediction result data respectively. Figure 7 showed the fitting curve of BPNN and GA-BPNN. In comparison, the predicted value of GA-BPNN fits better with the actual value, and the fluctuation is controlled in the range of $[-0.7, 1]$, while the predicted value of BPNN fluctuates slightly in the range of $[-1.3, 0.49]$. The analysis of the fitted data is given in the Table 6. By comparing the Figures 4 and 6, the improved network obviously shows that the prediction results are closer to the actual values and the fluctuations are reduced. The comparison between Figures 4 and 6 showed that the error range of the original network was $[-2.6, 2.3]$ and the error range of improved network was $[-1.9, 0.7]$. The improvement of the algorithm reduces the prediction error and the fluctuation of the values. Therefore the improvement of the network is effective.

Table 6. The fitted data.

	SSE	R-square	DFE	Adj R-sq	RMSE
BP Fitted Data	13.743795	0.993364	108	0.993302	0.488493
GA-BP Fitted Data	25.771643	0.996461	108	0.996428	0.356731

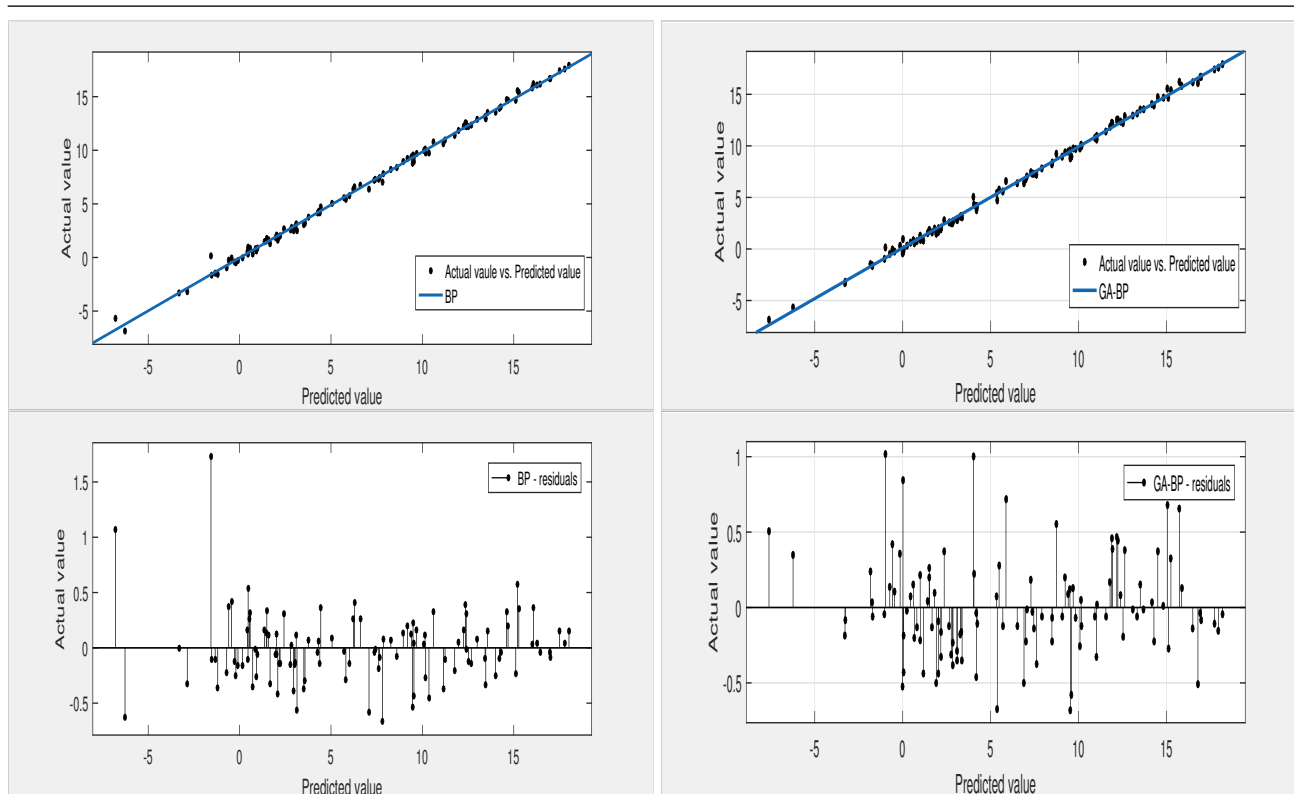


Figure 7. BP neural network and GA-BP neural network temperature prediction fitting curve.

4. The meteorological data screening experiments

In Section 3, we selected 8 different types of meteorological data as the input layer of the BP neural network to obtain the 8-9-1 neural network topology. In this section, we use the GA-BP neural network to select the best combination of data by choosing 6 out of 8 types of data as the input. Thus, the purpose of reducing the amount of input data is achieved. A total of $C_8^6 = 28$ ways to select 6 types of data out of 8 types of data. From Eq (3.1), the number of nodes in the hidden layer is taken to be in the range of [3,12]. By experimental simulation, the number of nodes in the hidden layer is set as 4. We conducted the prediction experiments in turn. The obtained results are given in the Table 7. In the Appendix, we presented the actual versus predicted curves of the test predictions for 28 experiments using GA-BPNN for a more visual display.

Combining the data in the following Table 7 and performing a comparative analysis, we can obtain that when MSLAP, RH, MWS, MAXG, MINT, and D-PT are selected as inputs, the values of each index can reach the best state. Among them, RMSE = 0.2705 and MAE = 0.20101 are less than 0.3. MAPE = 2.277 is the minimum value among 28 experiments. $R^2 = 0.99794$, which is close to 0.998. Through the experiment of influence factor selection, it can be seen that the choice of impact factors makes an impact towards the forecast value, and more influence factors may not be better, but partial data loss or too few influencing factors can increase the bias of the prediction. Therefore, when the data storage space is limited, the temperature prediction for the Laoshan scenic area can be carried out by preferentially selecting MSLAP, RH, MWS, MAXG, MINT, and D-PT.

Table 7. Operating parameters.

	RMSE	MAE	MAPE	R^2
RH,MWS,MAXG, MINT,HV,D-PT	0.57673	0.47115	35.8233	0.99322
MSLAP,MWS,MAXG, MINT,HV,D-PT	0.93737	0.75273	-6.5137	0.97607
MSLAP,RH,MAXG, MINT,HV,D-PT	0.28273	0.21147	-4.3979	0.99806
MSLAP,RH,MWS, MINT,HV,D-PT	0.46988	0.38296	3.4051	0.99448
MSLAP,RH,MWS,MAXG,HV,D-PT	0.41901	0.33745	6.8532	0.99703
MSLAP,RH,MWS, MAXG,MINT,D-PT	0.2705	0.20101	2.277	0.99794
MSLAP,RH,MWS,MAXG,MINT,HV	1.0247	0.81978	40.095	0.97037
HAP,MWS,MAXG,MINT,HV,D-PT	1.1576	0.91373	33.1758	0.96372
HAP,RH,MAXG, MINT,HV,D-PT	0.52654	0.44121	5.2227	0.99487
HAP,RH,MWS, MINT,HV,D-PT	0.46816	0.37099	-13.6055	0.99425
HAP,RH,MWS, MAXG,HV,D-PT	0.30757	0.24932	93.6903	0.99808
HAP,RH,MWS,MAXG,MINT,D-PT	0.452	0.37295	-50.7276	0.99558
HAP,RH,MWS,MAXG,MINT,HV	0.99626	0.78789	28.6812	0.97226
HAP,MSLAP,MAXG, MINT,HV,D-PT	0.90292	0.72788	11.6327	0.97788
HAP,MSLAP,MWS,MINT,HV,D-PT	0.99341	0.77745	24.9945	0.97342
HAP,MSLAP,MWS,MAXG,HV,D-PT	1.9731	1.5658	-257.2728	0.91054
HAP,MSLAP,MWS,MAXG,MINT,D-PT	1.0683	0.85061	9.6048	0.96837
HAP,MSLAP,MWS,MAXG,MINT,HV	1.0127	0.79219	30.9589	0.97262
HAP,MSLAP,RH,MINT,HV,D-PT	0.52593	0.43107	7.8321	0.99531
HAP,MSLAP,RH,MAXG,HV,D-PT	0.36603	0.28193	13.0585	0.99667
HAP,MSLAP,RH,MAXG,MINT,D-PT	0.44513	0.34116	11.4619	0.9948
HAP,MSLAP,RH,MAXG,MINT,HV	0.92494	0.71029	9.0949	0.97676
HAP,MSLAP,RH,MWS,HV,D-PT	0.44285	0.35799	18.1962	0.99594
HAP,MSLAP,RH,MWS,MINT,D-PT	0.32438	0.23941	-13.8789	0.99755
HAP,MSLAP,RH,MWS,MINT,HV	1.0187	0.80023	13.5466	0.97074
HAP,MSLAP,RH,MWS,MAXG,D-PT	0.34165	0.27842	17.295	0.99781
HAP,MSLAP,RH,MWS,MAXG,HV	1.2571	1.0156	40.6764	0.95651
HAP,MSLAP,RH,MWS,MAXG,MINT	0.83863	0.66808	90.157	0.98047

5. Conclusions and discussion

An improved genetic algorithm optimized BPNN, in this study is given for the temperature prediction problem. The optimization of genetic algorithm can, to some extent, avoid the neural network from falling into local extremes and enable the network to obtain better parameter settings. The simulation experiments of BP and GA-BP neural network prediction models were run several times using *Matlab* simulation program, respectively, and their parameters (RMSE, MAE, MAPE, R^2) were analyzed. It is obvious that the parameters in the improved network are set more scientifically and rationally. The R^2 value of GA-BP is stable within 0.98047–0.99823, and that of BP is stable within 0.97322–0.99745. Therefore the GA optimization method for the weights and thresholds of BPNN through the optimization-seeking operation is effective. From the simulation

results, the improvement work of this paper on the neural network can be concluded to have a positive impact on the prediction performance of the network.

In addition, through the screening of meteorological data parameters, this paper obtained six categories of meteorological parameters that have a large impact on temperature prediction. Analysis of the obtained RMSE, MAE, MAPE, and R^2 values can initially determine the magnitude of the influence of each type of meteorological parameters on temperature. In this paper, the analysis workload for meteorological data is large. Next we will analyze the meteorological data using more accurate and easy methods such as principal component analysis, cluster analysis methods [17].

Conflict of interest

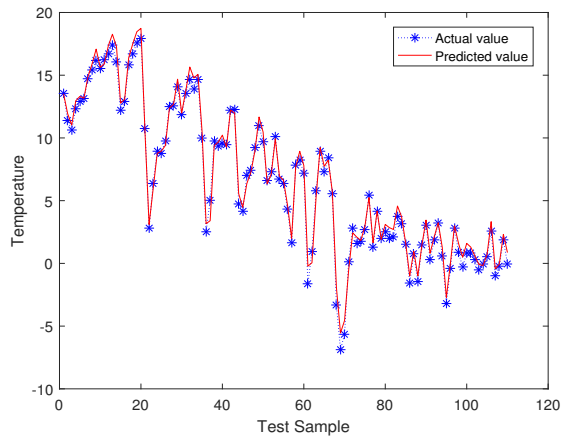
All authors declare no conflicts of interest in this paper.

References

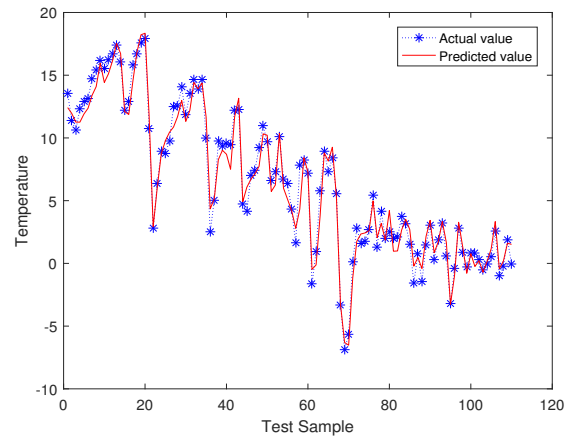
1. Khaniani AS, Motieyan H, Mohammadi A (2021) Rainfall forecast based on GPS PWV together with meteorological parameters using neural network models. *J Atmos Sol-Terr Phy* 214: 105533. <http://doi.org/10.1016/J.JASTP.2020.105533>
2. Huang H, Zhang JX, Song YP, et al. (2016) Prediction for quarterly precipitation in Xinjiang based on fuzzy time series prediction model. *Fuzzy Syst Math* 30: 176–182.
3. Lee J, Kim CG, Lee JE, et al. (2018) Application of artificial neural networks to rainfall forecasting in the Geum River basin, Korea. *Water* 10: 1448. <http://doi.org/10.3390/w10101448>
4. Liu Y, Zhao QZ, Yao WQ, et al. (2019) Short-term rainfall forecast model based on the improved BP–NN algorithm. *Sci Rep* 9: 19751. <http://doi.org/10.1038/s41598-019-56452-5>
5. Guan ZM, Tian ZY, Xu YS, et al. (2016) Rain fall predict and comparing research based on Arcgis and BP neural network. *2016 3rd international conference on materials engineering, manufacturing technology and control*, 1509–1514. <http://doi.org/10.2991/icmemtc-16.2016.291>
6. Peng YZ, Gong DQ, Deng CY, et al. (2022) An automatic hyperparameter optimization DNN model for precipitation prediction. *Appl Intell* 52: 2703–2719. <http://doi.org/10.1007/S10489-021-02507-Y>
7. Cho D, Yoo C, Son B, et al. (2022) A novel ensemble learning for post-processing of NWP Model's next-day maximum air temperature forecast in summer using deep learning and statistical approaches. *Weather Clim Extreme* 35: 100410. <http://doi.org/10.1016/J.WACE.2022.100410>
8. Shi JH, Yu J, Yang JK, et al. (2022) Time series surface temperature prediction based on cyclic evolutionary network model for complex sea area. *Future Internet* 14: 96. <http://doi.org/10.3390/FI14030096>
9. Song TY, Huang GH, Wang GQ, et al. (2022) Bayesian model averaging of the RegCM temperature projections: A Canadian case study. *J Water Clim Change* 13: 771–785. <http://doi.org/10.2166/WCC.2021.393>
10. Gupta S, Tripathi M, Grover J (2022) Hybrid optimization and deep learning based intrusion detection system. *Comput Electr Eng* 100: 107876. <http://doi.org/10.1016/J.COMPELECENG.2022.107876>

11. Lei YS, Cai XJ, Wang W (2018) Application research of BP neural network optimized by genetic algorithm in multi-model ensemble forecast about ground temperature. *J Meteorol Sci* 38: 806–814.
12. Yao C, Jin L, Huang MC, et al. (2007) An experiment with methods of forecasting tropical cyclones intensity base on combination of the genetic algorithm and artificial neural network. *Acta Oceanol Sin* 29: 11–19.
13. Wu JS (2016) Hybrid optimization algorithm to combine neural network for rainfall-runoff modeling. *Int J Comput Intell* 15: 1650015. <http://doi.org/10.1142/S1469026816500152>
14. Sun T, Chen YD, Meng DM, et al. (2021) Background error covariance statistics of hydrometeor control variables based on gaussian transform. *Adv Atmos Sci* 38: 831–844. <http://doi.org/10.1007/S00376-021-0271-3>
15. Tang SZ, Li MJ, Wang FL, et al. (2020) Fouling potential prediction and multi-objective optimization of a flue gas heat exchanger using neural networks and genetic algorithms. *Int J Heat Mass Tran* 152: 119488. <http://doi.org/10.1016/j.ijheatmasstransfer.2020.119488>
16. Liu CH, Yang L, Deng H, et al. (2019) Prediction of ammonia concentration in piggery based on ARIMA and BP neural network. *China Environ Sci* 39: 2320–2327. <http://doi.org/10.19674/j.cnki.issn1000-6923.2019.0276>
17. Xie YQ, Ishidal Y, Hu JL, et al. (2022) A backpropagation neural network improved by a genetic algorithm for predicting the mean radiant temperature around buildings within the long-term period of the near future. *Build Simul* 15: 473–492. <http://doi.org/10.1007/S12273-021-0823-6>

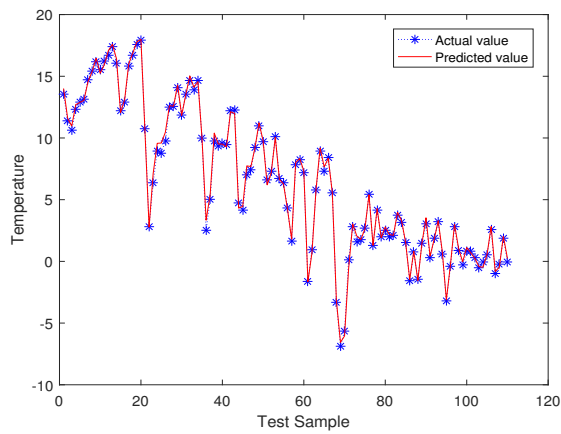
Appendix



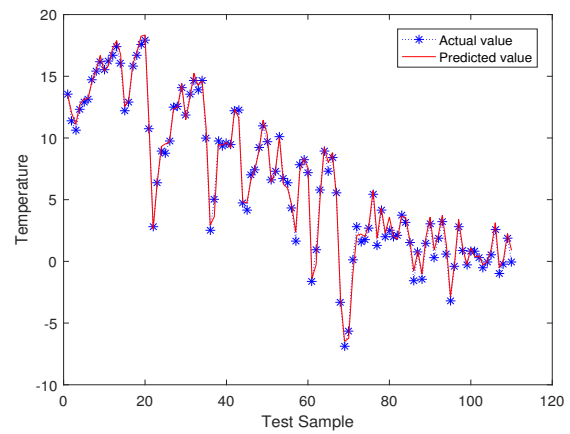
(a) RH,MWS,MAXG, MINT,HV,D-PT



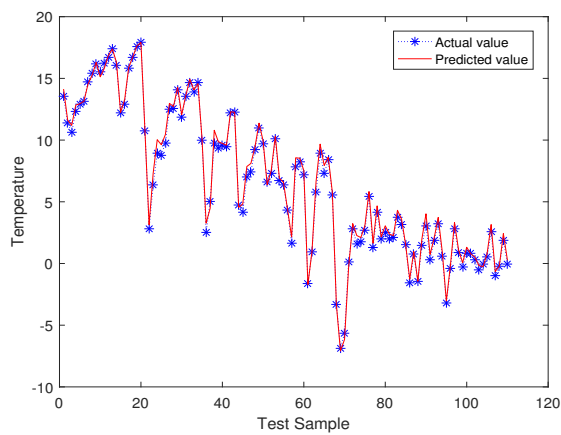
(b) MSLAP,MWS,MAXG, MINT,HV,D-PT



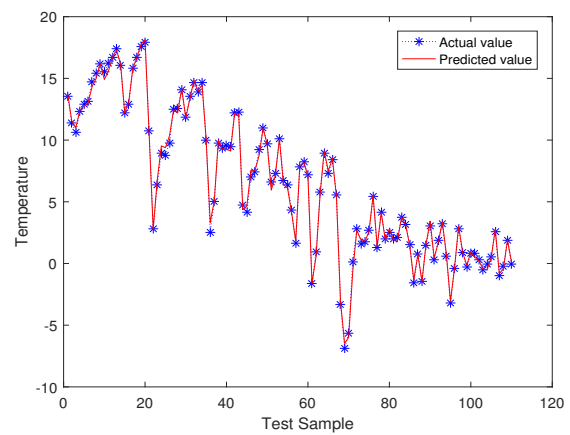
(c) MSLAP,RH,MAXG, MINT,HV,D-PT



(d) MSLAP,RH,MWS, MINT,HV,D-PT

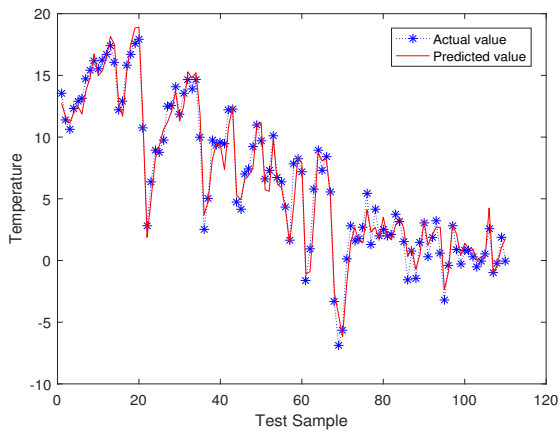


(e) MSLAP,RH,MWS,MAXG,HV,D-PT

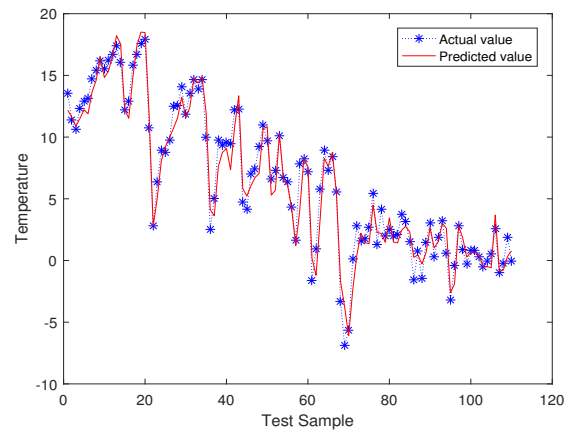


(f) MSLAP,RH,MWS, MAXG,MINT,D-PT

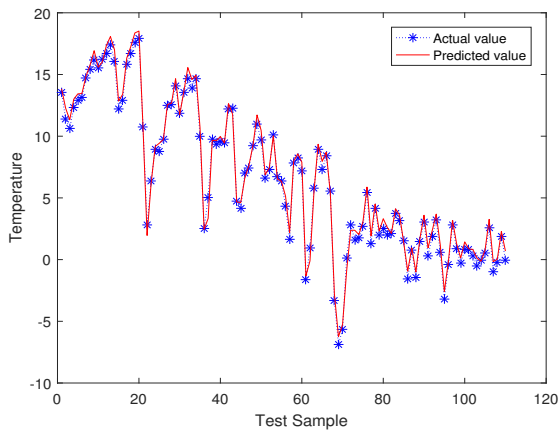
Figure 8. The GA-BPNN prediction curve when 6 types of parameters.



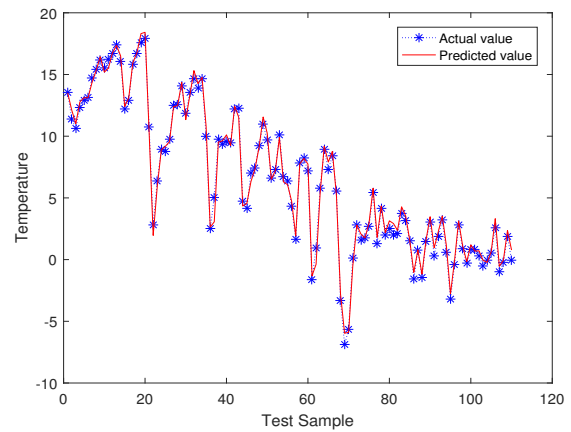
(a) MSLAP,RH,MWS,MAXG,MINT,HV



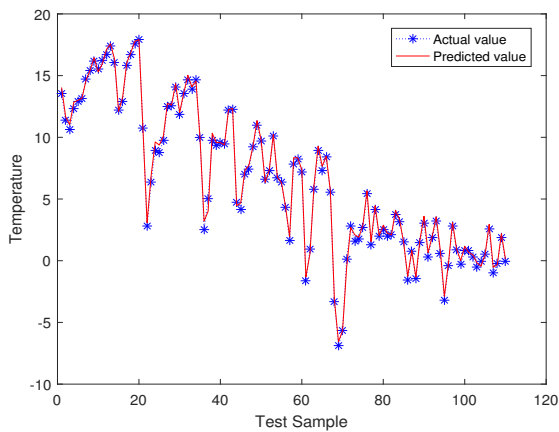
(b) HAP,MWS,MAXG,MINT,HV,D-PT



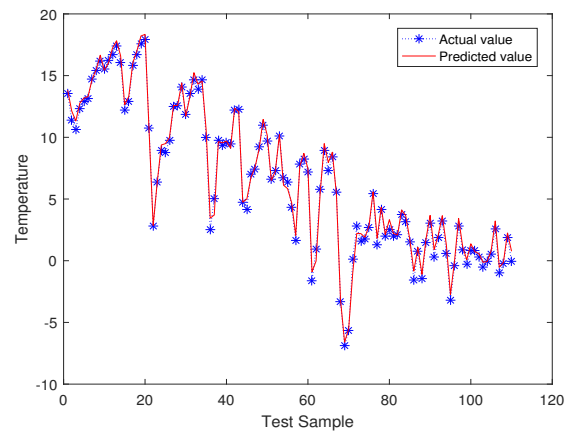
(c) HAP,RH,MAXG, MINT,HV,D-PT



(d) HAP,RH,MWS, MINT,HV,D-PT

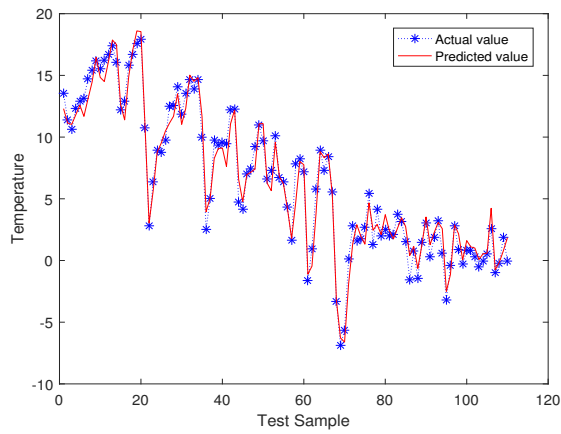


(e) HAP,RH,MWS, MAXG,HV,D-PT

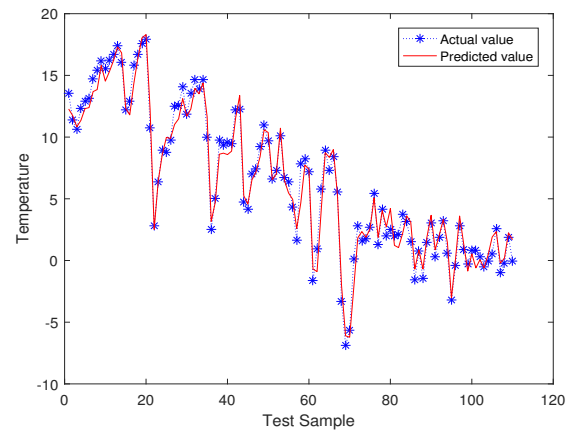


(f) HAP,RH,MWS,MAXG,MINT,D-PT

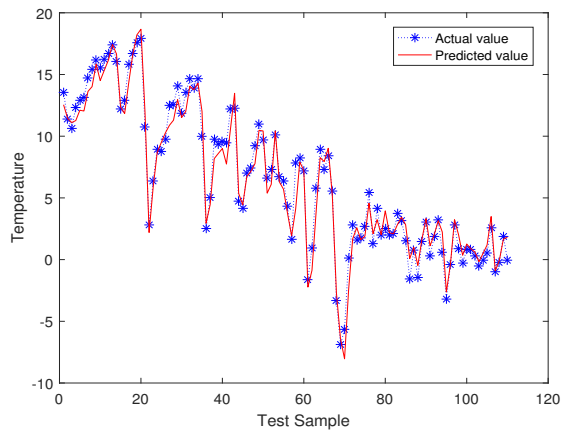
Figure 9. The GA-BPNN prediction curve when 6 types of parameters.



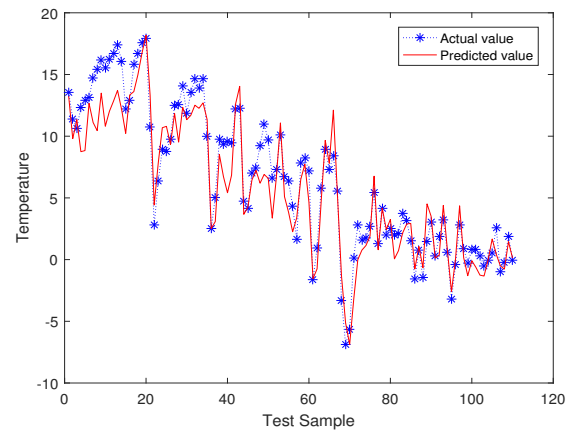
(a) HAP,RH,MWS,MAXG,MINT,HV



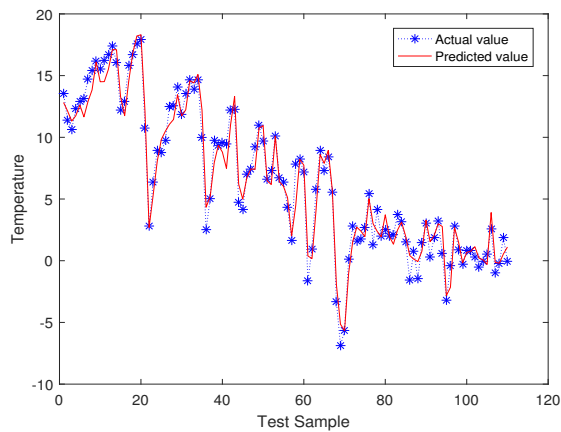
(b) HAP,MSLAP,MAXG, MINT,HV,D-PT



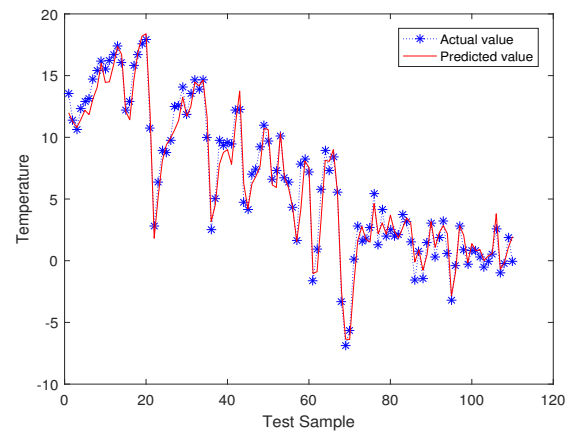
(c) HAP,MSLAP,MWS,MINT,HV,D-PT



(d) HAP,MSLAP,MWS,MAXG,HV,D-PT

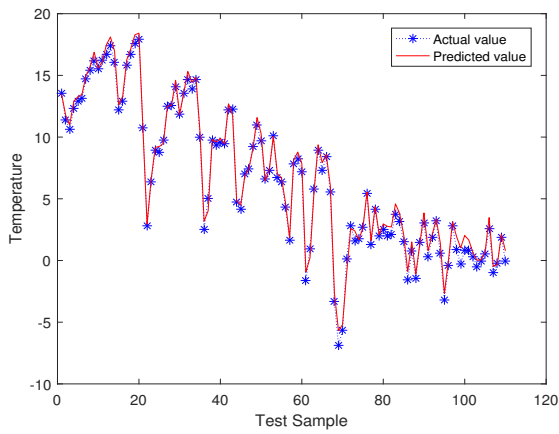


(e) HAP,MSLAP,MWS,MAXG,MINT,D-PT

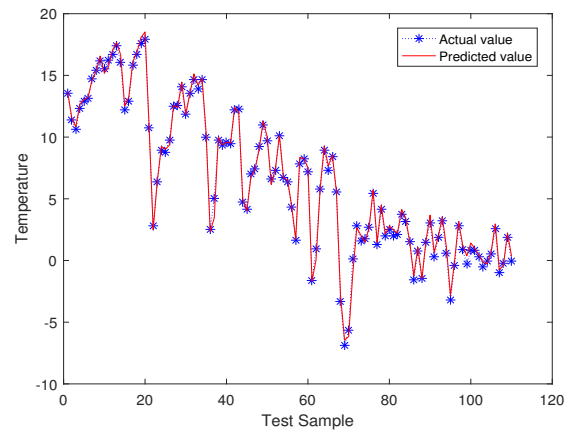


(f) HAP,MSLAP,MWS,MAXG,MINT,HV

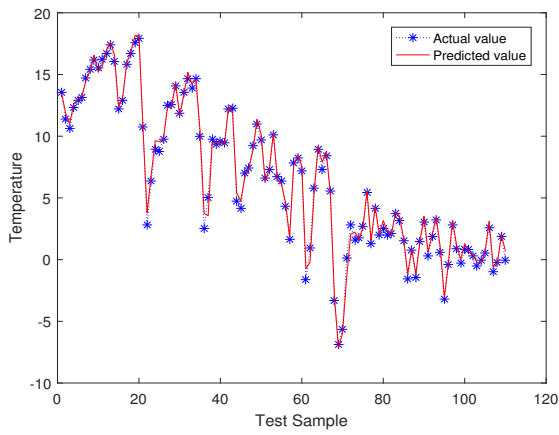
Figure 10. The GA-BPNN prediction curve when 6 types of parameters.



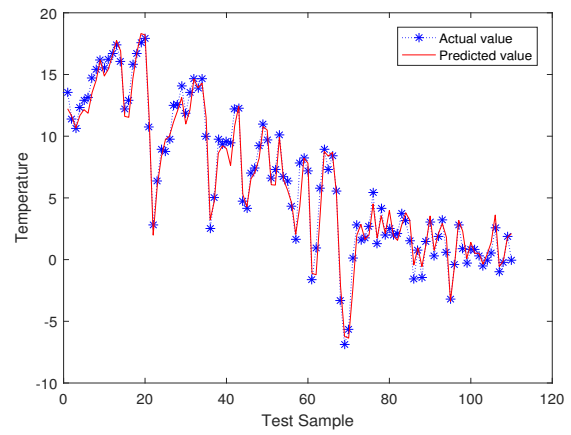
(a) HAP,MSLAP,RH,MINT,HV,D-PT



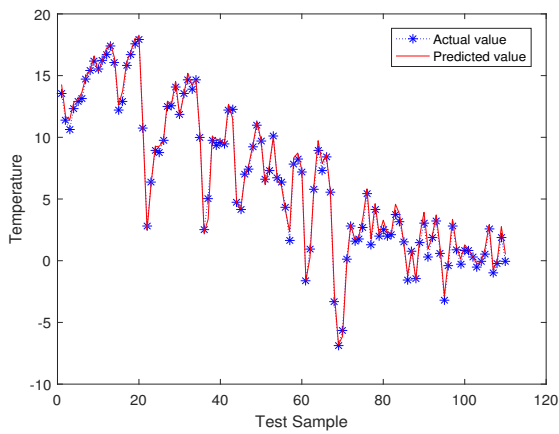
(b) HAP,MSLAP,RH,MAXG,HV,D-PT



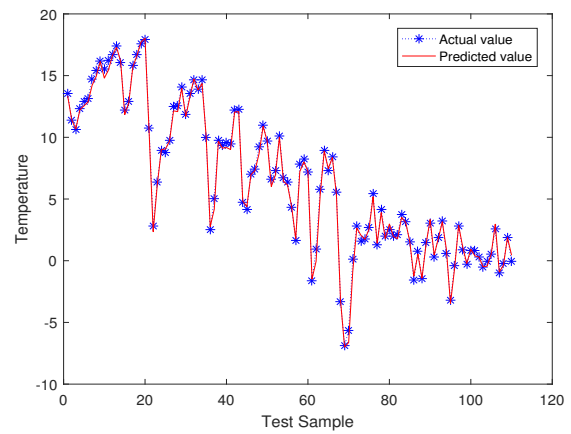
(c) HAP,MSLAP,RH,MAXG,MINT,D-PT



(d) HAP,MSLAP,RH,MAXG,MINT,HV

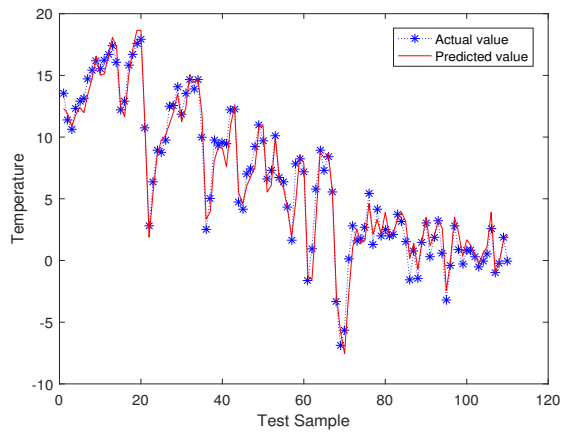


(e) HAP,MSLAP,RH,MWS,HV,D-PT

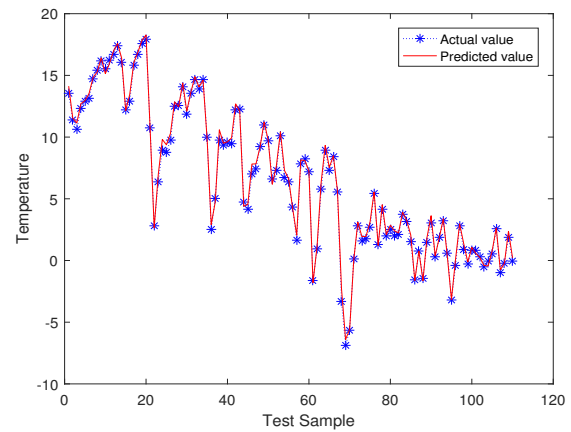


(f) HAP,MSLAP,RH,MWS,MINT,D-PT

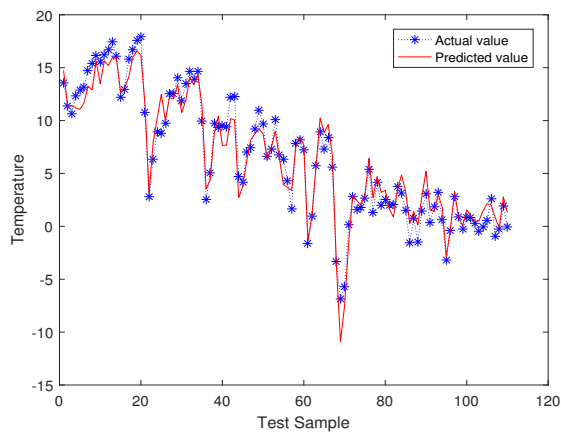
Figure 11. The GA-BPNN prediction curve when 6 types of parameters.



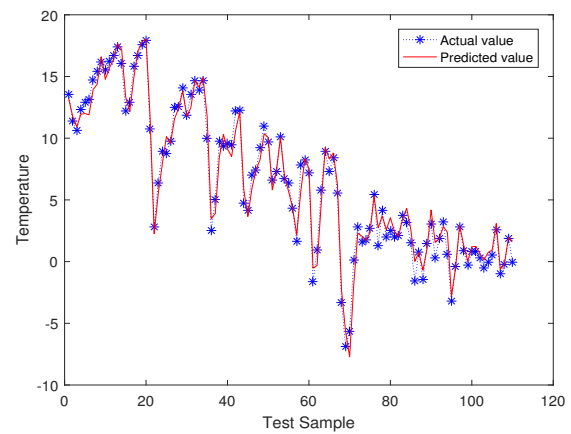
(a) HAP,MSLAP,RH,MWS,MINT,HV



(b) HAP,MSLAP,RH,MWS,MAXG,D-PT



(c) HAP,MSLAP,RH,MWS,MAXG,HV



(d) HAP,MSLAP,RH,MWS,MAXG,MINT

Figure 12. The GA-BPNN prediction curve when 6 types of parameters.



AIMS Press

© 2022 the Author(s), licensee AIMS Press. This is an open access article distributed under the terms of the Creative Commons Attribution License (<http://creativecommons.org/licenses/by/4.0>)